



HAL
open science

Numerical simulation of a swirl stabilized methane-air flame with an automatic meshing CFD solver

Lorenzo Palanti, Daniele Pampaloni, Antonio Andreini, Bruno Facchini

► **To cite this version:**

Lorenzo Palanti, Daniele Pampaloni, Antonio Andreini, Bruno Facchini. Numerical simulation of a swirl stabilized methane-air flame with an automatic meshing CFD solver. *Energy Procedia*, 2018, 148, pp.376-383. 10.1016/j.egypro.2018.08.098 . hal-02127949

HAL Id: hal-02127949

<https://normandie-univ.hal.science/hal-02127949v1>

Submitted on 3 Jun 2024

HAL is a multi-disciplinary open access archive for the deposit and dissemination of scientific research documents, whether they are published or not. The documents may come from teaching and research institutions in France or abroad, or from public or private research centers.

L'archive ouverte pluridisciplinaire **HAL**, est destinée au dépôt et à la diffusion de documents scientifiques de niveau recherche, publiés ou non, émanant des établissements d'enseignement et de recherche français ou étrangers, des laboratoires publics ou privés.



Distributed under a Creative Commons Attribution - NonCommercial - NoDerivatives 4.0 International License



73rd Conference of the Italian Thermal Machines Engineering Association (ATI 2018), 12-14 September 2018, Pisa, Italy

Numerical simulation of a swirl stabilized methane-air flame with an automatic meshing CFD solver

Lorenzo Palanti^{a,*}, Daniele Pampaloni^a, Antonio Andreini^a, Bruno Facchini^a

^a*Department of Industrial Engineering, University of Florence, Via di S. Marta, 3, Firenze 50139, Italy*

Abstract

The reliable prediction of the turbulent combustion processes in lean flames is nowadays of crucial importance in the design of gas turbine combustors. This work presents an assessment of the capabilities of Flamelet Generated Manifold (FGM) in the framework of Large-Eddy Simulation (LES), as implemented in the commercial CFD solver CONVERGE. One of the main characteristic of the code is the Adaptive Mesh Refinement (AMR) technique, namely the use of a dynamic mesh where elements size varies during the simulation. For validation purposes, the TECFLAM swirl burner, consisting of a strongly swirling, unconfined natural gas flame, has been chosen. Results highlight the advantages of AMR in describing turbulent flames, leading to a successful prediction of the main characteristics of the reacting flow field.

© 2018 The Authors. Published by Elsevier Ltd.

This is an open access article under the CC BY-NC-ND license (<https://creativecommons.org/licenses/by-nc-nd/4.0/>)

Selection and peer-review under responsibility of the scientific committee of the 73rd Conference of the Italian Thermal Machines Engineering Association (ATI 2018).

Keywords: Gas turbine; Combustion; Swirl flame; Methane; CFD; LES; Adaptive Mesh Refinement; FGM.

1. Introduction

Lean swirling flames are widely used in technical applications such as power generation systems and heavy-duty gas turbines. The main aim of such technology is to provide a consistent reduction of the nitrogen oxides (NO_x) emissions by strictly controlling the equivalence ratio and therefore the combustion temperature. As an alternative to very expensive and time consuming experimental investigations, computational methods can be used to predict burner performances and investigate flame behavior. Nowadays, Large-Eddy Simulation (LES) is achieving a growing attention for its accuracy in reproducing the turbulent flowfield and has been already widely employed for the simulation of both premixed and non-premixed gaseous flames [5]. Regarding the combustion modelling, approaches characterized by a detailed description [5] of the chemical kinetics are required. In this framework, the Flamelet Generated Manifold (FGM) model has proven to be able of accurately reproducing the complex topology and the stabilization mechanism

*Corresponding author. Tel.: +39-055-275-8771.

E-mail address: lorenzo.palanti@unifi.it

of lean burn flames [18, 17], despite the low computational costs. In the present work, the TECFLAM swirl burner, a natural gas swirling unconfined flame, has been studied employing the FGM to model turbulent combustion in a LES framework. The presented simulation has been performed employing the commercial CFD solver CONVERGE developed by Convergent Science [11]. One of the main characteristic of such code is the Adaptive Mesh Refinement (AMR) technique: it aims at overcoming all the problems linked to the use of a static grid by introducing a dynamic mesh where elements size varies during the simulation. Firstly, an orthogonal hexahedral base grid is automatically generated based on a few user-defined control parameters and fixed embedding is possible in the regions of interest, for instance inside the nozzle or close to the walls. During the simulation, the mesh is automatically refined in the regions where the second derivative of user defined variables is higher than a certain threshold. Such technique allows a strong reduction of the computational cost while keeping a high-fidelity prediction of the main flow quantities. The objective of this work is to preliminary validate the numerical setup and show the capabilities of AMR in describing turbulent swirling partially-premixed flames.

Nomenclature

S	Grid sizing
ϕ	General scalar
AMR	Adaptive Mesh Refinement
CFD	Computational Fluid Dynamics
FGM	Flamelet Generated Manifold
LES	Large-Eddy Simulation

2. Experimental test case

The test case presented here is a further development of the configurations defined within the TECFLAM (TECHnical FLAMes) project of the Institute of Combustion and Power Plant Technology and consists of a strongly swirled unconfined gaseous flame [13, 6]. The aim of such effort was to define a standard natural gas swirl burner and perform high-level quantitative measurements to achieve a complete characterization of the flame. Measurements of the velocity (mean and standard deviation) were performed in [13] using Laser Doppler Anemometry while in [6] Raman/Rayleigh scattering has been used to estimate the major species and the temperature distribution.

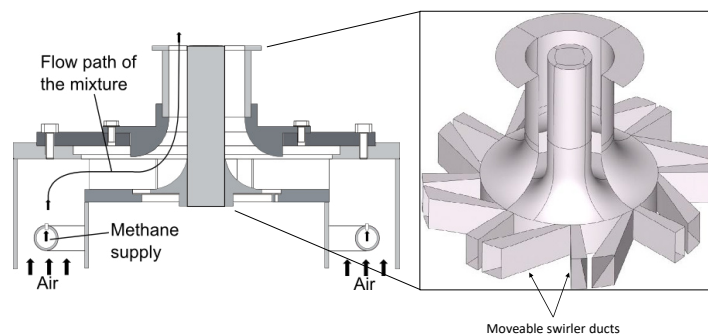


Fig. 1. Schematic view of the TECFLAM burner (adapted from [7])

Swirl number has been set to 0.75 by adjusting the moveable geometry of the swirler ducts (Figure 1). Swirl number is high enough to establishing a central recirculation zone due to vortex breakdown. In reactive conditions, it enforces the backflow of hot gases towards the nozzle and is responsible for flame stabilisation. In Figure 1 the air enters from the bottom and natural gas is injected using a pressurized perforated ring line. The produced mixture (air

and methane with equivalence ratio of 0.83) is then deflected by 90 and splitted through radial and tangential channels. Then, it flows inside the annulus around the bluff body, which is water-cooled in order to maintain a temperature of 353 K, and finally enters the unconfined section. Here, it is surrounded by a slow co-axial air flow (0.5 m/s), injected from a concentric annular orifice. Experimental investigations were carried out in three different operating conditions, corresponding to three level of thermal power, namely 30, 90, 150 kW [3]. In this work the lower level has been investigated and the most relevant conditions are summarised in Table 1. It should be noticed that Reynolds number is calculated based on the flow conditions at the exit plane of the nozzle using the diameter of central bluff body.

Table 1. Investigated flow conditions

Data	Unit	Value
Swirl number	[-]	0.75
Thermal power	[kW]	30
Equivalence ratio	[-]	0.83
Reynolds number	[-]	10.000

3. Meshing strategy

Most of the CFD software require time-consuming manual mesh generation and, when available, a tricky setup of their automated meshing features. As result of that, the time required by the user to generate the computational grid is often a large part of the overall amount employed to set up the case. To overcome this issue, CONVERGE integrates a tool that automatically generates an orthogonal grid at runtime, based on a few user-defined grid control parameters, allowing a consistent speed up of the case setup. A modified cut-cell cartesian method is implemented [14] which eliminates the need to shape the computational grid over the geometry of interest, while the true boundary morphology is still precisely described. To completely take advantage of such automatic meshing feature a run time adaptive mesh refinement is available in CONVERGE. In fact, thanks to the hexahedral shape of the elements, AMR is of straightforward application: given an element with an certain initial size (S_{pre}) the grid is embedded by splitting it into smaller elements, characterized by a size of S_{post} (Equation 1) where n is an integer.

$$S_{post} = \frac{S_{pre}}{2^n} \quad (1)$$

The main aim of such algorithm is to increase the grid resolution in the regions where the flow is particularly complex, whereas leaving the mesh relatively coarse in less critical sections. Since it is difficult to determine a priori where a local refinement is required, considering that in unsteady simulations these zones may vary due to turbulent instabilities, a general criterion is required to determine whether the grid must be embedded or not. In CONVERGE, such criterion is based on the estimation of the magnitude of the sub-grid field of a certain user-specified variable (e.g. temperature and velocity magnitude in Figure 2). Considering a general scalar ϕ , the sub-grid field (ϕ') is defined as the difference between the actual and the resolved field ($\bar{\phi}$), $\phi' = \phi - \bar{\phi}$. According to [2, 4] the sub-grid field can be expressed as an infinite series:

$$\phi' = -\alpha_{[k]} \frac{\partial^2 \bar{\phi}}{\partial x_k \partial x_k} + \frac{1}{2!} \alpha_{[k]} \alpha_{[l]} \frac{\partial^4 \bar{\phi}}{\partial x_k \partial x_k \partial x_l \partial x_l} - \frac{1}{3!} \alpha_{[k]} \alpha_{[l]} \alpha_{[m]} \frac{\partial^6 \bar{\phi}}{\partial x_k \partial x_k \partial x_l \partial x_l \partial x_m \partial x_m} + \dots \quad (2)$$

where $\alpha_{[k]} = dx_k^2/24$ for a rectangular cell and the brackets [] indicate no summation. Since it is not possible to evaluate the entire series, only the first term (the second-order term) of the series is used to approximate the scale of the sub-grid, namely:

$$\phi' \cong -\alpha_{[k]} \frac{\partial^2 \bar{\phi}}{\partial x_k \partial x_k} \quad (3)$$

From the expression above it is clear that the AMR is based on the second derivative of the involved scalar. The same approach has been extended to vector fields, in order to allow AMR on velocity also.

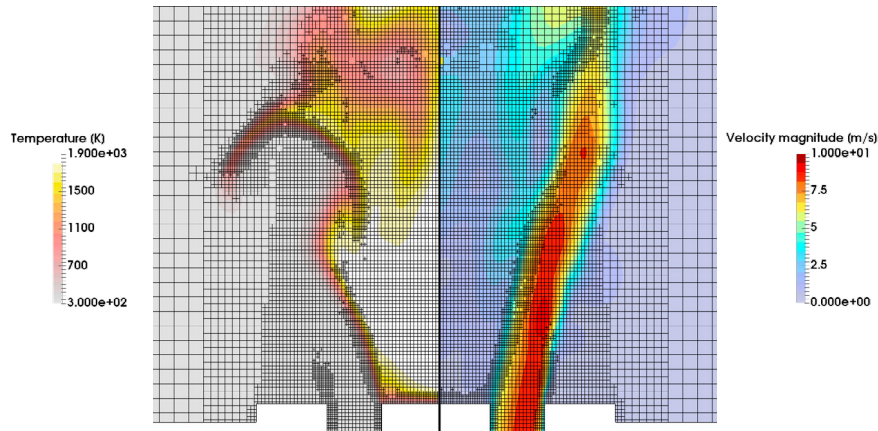


Fig. 2. Example of adaptive mesh refinement in CONVERGE driven by temperature and velocity variation respectively

Finally, a threshold value is required to establish if the element will be embedded or not: a cell is embedded if the absolute value of the sub-grid field is above it. The choice of such value is based on user experience, available computational resources and the adopted turbulence model. In fact, the lower the value of the threshold, the higher the mesh resolution and therefore the number of elements. For instance, it is obvious that LES will require higher mesh resolution with respect to RANS and therefore a lower value of AMR threshold. Typical ranges of such parameter for standard variables are reported in Table 2.

Table 2. Recommended ranges for sub-grid criterion [12]

Field	Recommended value
Velocity	0.1% to 10% of characteristic velocity in the domain.
Temperature	0.1% to 10% of characteristic temperature in the domain.

In order to save computational resources, AMR is normally applied only when the flow is completely developed in the domain (i.e. when the initialization has been completely flushed). To achieve a proper mesh resolution in critical regions, such as the narrow channels of the swirler, fixed embedding has been introduced. Similarly to other CFD solvers, it allows a local refinement of the mesh, independent from flow characteristics, to guarantee a more appropriate flow and geometry description, while keeping low the number of elements in regions of less interest.

4. Numerical setup

The Smagorinsky model [15] has been employed to model the sub-grid stress tensor which appears from the filtered system of Navier-Stokes equations of a turbulent flow field. A Werner Wengle wall model [20] has been used to reproduce fluid-wall interactions and boundary layers. The combustion process has been modeled through a Flamelet Generated Manifold (FGM) approach [8] where the mean source term of the reaction progress has been closed with the turbulent flame speed closure proposed by Zimont [21]. GRI Mech 3.0 chemistry [16] for methane combustion has been employed to generate the manifold data. The tabulated chemistry has been sampled from a set of 1D freely propagating premixed flames solved in physical space over the entire range of equivalence ratios. The results from the flamelets solution have been then stored in a look-up table to be used during the CFD computation. The computational domain used in the reported simulation is composed by the combustion chamber, the swirler and an annular plenum chamber which feeds the entire device with fresh mixture (Figure 3). Such plenum has been included in the numerical domain, as already done in other works [19, 1] in order to fully evaluate the automatic meshing features of CONVERGE and its capability of reproducing the effective flow field. On the other hand, directly impose the air flow split

in tangential and radial channels provide a tighter control on the swirl number [10] and ensure the aforementioned experimental conditions to be matched.

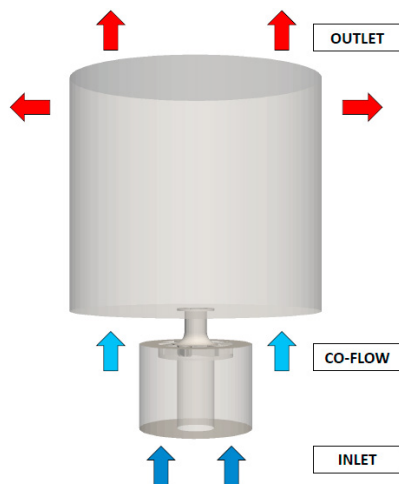


Fig. 3. Computational domain tested in this work

Regarding the inlet boundary condition, the main assumptions are listed in Table 3. It should be highlighted that no artificial turbulence has been added at the inlet, since the main eddies are normally generated across the swirler.

Table 3. Relevant boundary conditions

Data	Unit	Inlet	Co-flow
Mass flow rate	[kg/s]	0.1313	-
Axial velocity	[m/s]	-	0.5
Temperature	[K]	300	300
Mean progress variable	[-]	0	0
Mean mixture fraction	[-]	1	0
Variance of the mixture fraction	[-]	0	0

At the outlet surfaces, a fixed pressure of 101325 [Pa] has been set to mimic ambient conditions. No-slip condition and imposed temperature (353 K) have been imposed on all the walls of the domain. A second order central differencing approximation scheme has been used for momentum, energy, density, mixture fraction (mean and variance) and mean progress variable. Transport equations have been solved using the PISO algorithm [9]: throughout this work the simulation time step has been automatically set according to a maximum value of Courant-Friedrichs-Lewy number, placed equal to one. A base grid size of 8 mm has been employed with a maximum embedding level of 4: the resulting minimum element size is 500 μm . AMR has been based on velocity and temperature sub-grid fields, with a threshold value of 0.09 m/s and 50 K respectively.

5. Results and discussion

In combustion applications the use of LES generally leads to a drastic improvement in the predicted results with respect to RANS (for instance in [10]). Preliminary RANS simulations have been performed but for the sake of brevity they are not reported here. Moreover, an interesting feature of the automatic meshing method implemented in CONVERGE is that preliminary simulation are no longer required to initialize the LES flow field. In fact, the initial solution can be flushed out with a coarser mesh which can be refined on the fly during the same run. In present study for instance, a first coarser grid has been generated to allow the methane to quickly fill the combustion chamber. Then, the mixture has been ignited using a volumetric energy and mean progress variable source term. After flame propagation

and stabilization, AMR has been activated, together with a further embedding in the near field of the nozzle, leading to an average number of elements of about 7 M. This strategy allows to strongly reduce the computational effort required to initialize unsteady simulations, achieving at the same time a very high mesh resolution at the end of the simulation. Results shown hereby are obtained by averaging in time the turbulent unsteady flow field. Comparisons with experiments have been carried out over some planes, highlighted in Figure 4.

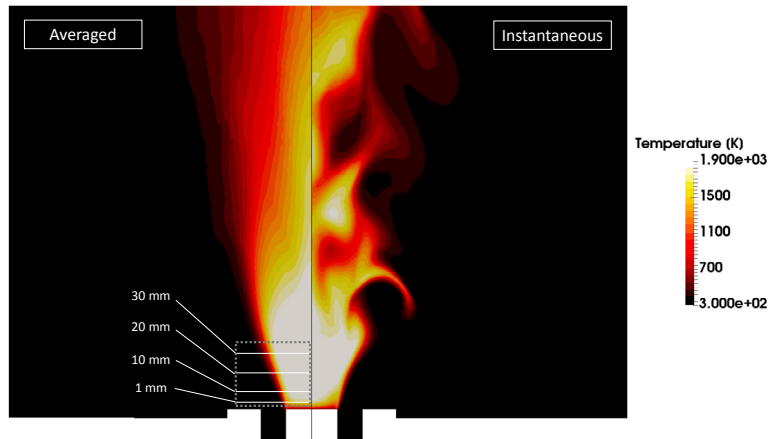


Fig. 4. Averaged and instantaneous temperature field superimposed with employed sampling planes

By defining x as the axial distance from swirler nozzle, the velocity flow field has been investigated at $x = 1, 10, 20, 30 \text{ mm}$. Instead, temperature has been compared, using a reduced number of planes, placed at $x = 10, 20, 30 \text{ mm}$.

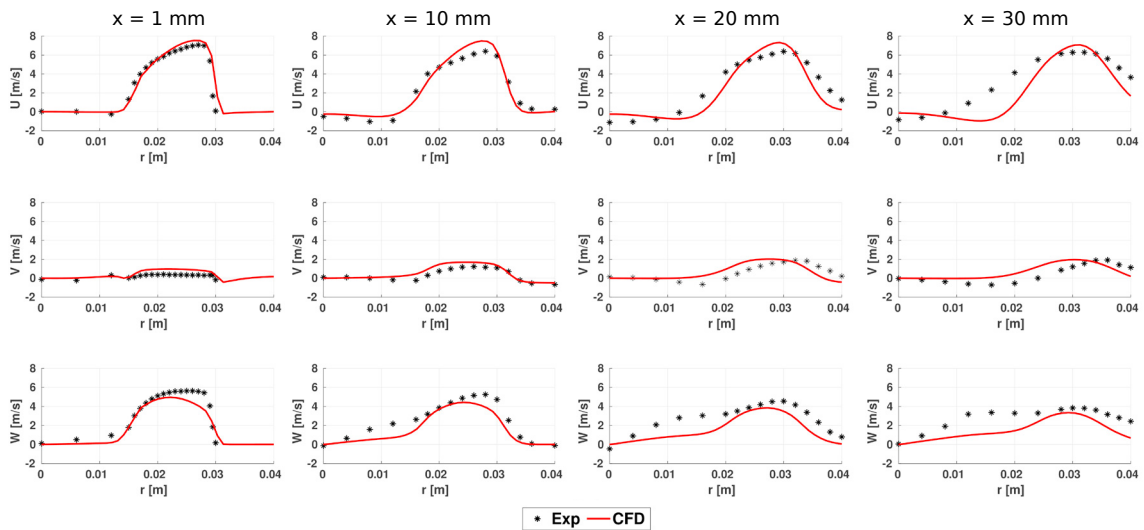


Fig. 5. Comparison of axial, radial and tangential velocity with experimental data

A general good agreement can be observed in the profiles of velocity reported in Figure 5. At the nozzle exit ($x = 1 \text{ mm}$) all the velocity components are well matched, demonstrating that the selected setup is capable of correctly reproduce the flow field inside the nozzle. Moving downstream the combustion chamber, the swirled flow starts to spread outwards and, as effect of this, the axial velocity peak starts to move towards higher radii. Tangential velocity, which is higher for $x = 1 \text{ mm}$, rapidly decays as it is converted into radial one, allowing the flow spreading mentioned

above. This behaviour is well matched by the simulation. At $x = 30 \text{ mm}$ the axial velocity peak is slightly overestimated but it decays more rapidly moving inward and outward. This could be due to a poor representation of the mixing promoted by turbulence which can be enhanced by a further refinement of the grid to allow more turbulent structures to be resolved.

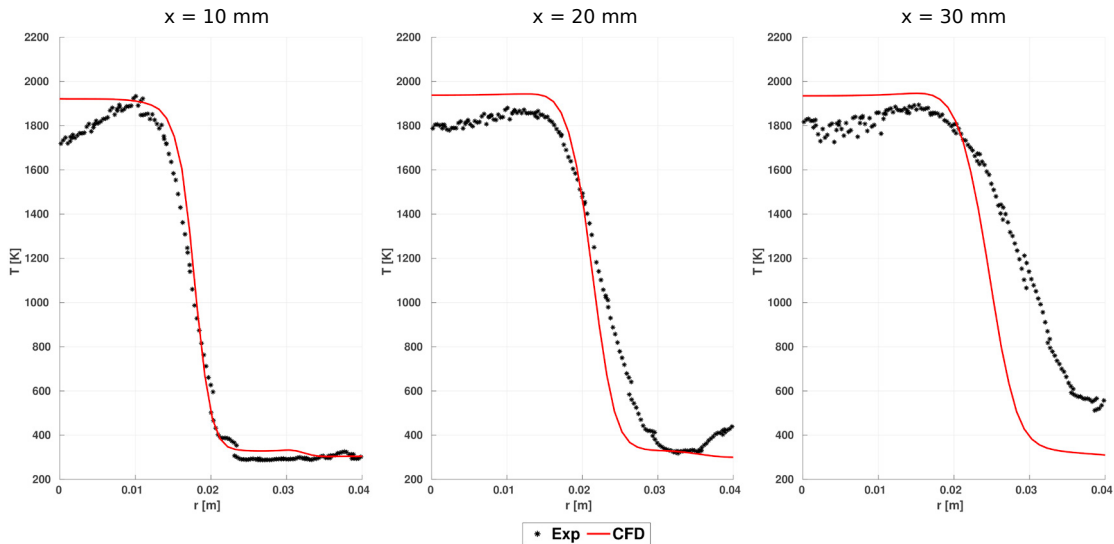


Fig. 6. Comparison of temperature with experimental data

Regarding the comparison of the temperature profiles, at $x = 10 \text{ mm}$ the maximum peak and the steep drop are well represented by the simulation. Nevertheless, the temperature on the swirler axis is well over predicted. This is probably the effect of a poor description of intermittent nature of the turbulent flow and the heat losses promoted by long residence times inside the inner recirculation zone. At $x = 20 \text{ mm}$ and $x = 30 \text{ mm}$ the same behaviour can be identified. Moreover, for what concerns experimental results, the temperature gradient is flattened as the width of the flame brush is increased by turbulence in axial direction [6]. Such thickening is not recovered in simulation, as the temperature profile has the same slope in all the three sampling planes. As stated for before, a better description of turbulent structures in such zone can be achieved by locally refining the mesh or by imposing a lower threshold value for the AMR. Furthermore, these discrepancies can probably be overcome by a finer tuning of the prefactor coefficient used in Zimont correlation, but this analysis was out of the scope of this work.

6. Conclusions

LES calculation of a swirler stabilized lean-burn flame has been performed using AMR techniques. The comparison with experimental data shows the improvements that can be obtained in describing turbulent flames modifying the grid size during the simulation in order to achieve the required accuracy only in the regions of interest while keeping low the overall computational effort.

Acknowledgements

We would like to thank Federico Fantoni, one of our former students, since this work is an extract of his master thesis. We gratefully acknowledge the Convergent Science company for providing the CONVERGE software and their precious support to run the simulations. The authors would also like to thank Prof. Andreas Dreizler for sharing geometry and experimental data of the TECFLAM test case.

References

- [1] Amsini, S., Maltsev, A., Wegner, B., Flemming, F., Kempf, A., Janicka, J., 2006. Unsteady methods (urans and les) for simulation of combustion systems. *International Journal of Thermal Sciences* 45, 760–773.
- [2] Bedford, K., Yeo, W., 2010. Conjunctive filtering procedures in surface water flow and transport. *Large eddy simulation of complex engineering and geophysical flows*, 513–537.
- [3] Butz, D., Gao, Y., Kempf, A., Chakraborty, N., 2015. Large eddy simulations of a turbulent premixed swirl flame using an algebraic scalar dissipation rate closure. *Combustion and Flame* 162.
- [4] Eric, P., 2000. Development of large eddy simulation turbulence models. Ph.D. thesis. University of Wisconsin–Madison.
- [5] Gicquel, L., Staffelbach, G., Poinot, T., 2012. Large eddy simulations of gaseous flames in gas turbine combustion chambers. *Progress in Energy and Combustion Science* 38.
- [6] Gregor, M., Seffrin, F., Fuest, F., Geyer, D., Dreizler, A., 2009. Multi-scalar measurements in a premixed swirl burner using 1d raman/rayleigh scattering. *Proceedings of the Combustion Institute* 32, 1739–1746.
- [7] Kuenne, G., Ketelheun, A., Janicka, J., 2011. Les modeling of premixed combustion using a thickened flame approach coupled with fgm tabulated chemistry. *Combustion and Flame* 158, 1750 – 1767.
- [8] Oijen, J.v., Goey, L.d., 2000. Modelling of premixed laminar flames using flamelet-generated manifolds. *Combustion Science and Technology* 161, 113–137.
- [9] Oliveira, P., Issa, R., 2001. An improved piso algorithm for the computation of buoyancy-driven flows. *Numerical Heat Transfer: Part B: Fundamentals* 40, 473–493.
- [10] Pampaloni, D., Bertini, D., Puggelli, S., Mazzei, L., Andreini, A., 2017. Methane swirl-stabilized lean burn flames: assessment of scale-resolving simulations. *Energy Procedia* 126, 834 – 841. ATI 2017 - 72nd Conference of the Italian Thermal Machines Engineering Association.
- [11] Richards, K., Senecal, P., Pomraning, E., 2017a. Converge (2.4), convergent science. Inc., Madison, WI .
- [12] Richards, K., Senecal, P., Pomraning, E., 2017b. Converge 2.4 manual, convergent science. Inc., Madison, WI .
- [13] Schneider, C., Dreizler, A., Janicka, J., 2005. Fluid dynamical analysis of atmospheric reacting and isothermal swirling flows. *Flow, turbulence and combustion* 74, 103–127.
- [14] Senecal, P., Richards, K., Pomraning, E., Yang, T., Dai, M., McDavid, R., Patterson, M., Hou, S., Shethaji, T., 2007. A new parallel cut-cell cartesian cfd code for rapid grid generation applied to in-cylinder diesel engine simulations. *SAE Technical Paper* .
- [15] Smagorinsky, J., 1963. General circulation experiments with the primitive equations: I. the basic experiment. *Monthly weather review* 91, 99–164.
- [16] Smith, G., Golden, M., Frenklach, M., Moriarty, N., Eiteneer, B., Goldenberg, M., Bowman, C., Hanson, R., Song, S., Gardiner Jr, W., et al., 1999. Gri 3.0 mechanism. Gas Research Institute, Des Plaines, IL, accessed Aug 21, 2017.
- [17] Van Oijen, J., Donini, A., Bastiaans, R., ten Thije Boonkkamp, J., De Goey, L., 2016. State-of-the-art in premixed combustion modeling using flamelet generated manifolds. *Progress in Energy and Combustion Science* 57, 30–74.
- [18] Van Oijen, J., Lammers, F., De Goey, L., 2001. Modeling of complex premixed burner systems by using flamelet-generated manifolds. *Combustion and Flame* 127, 2124–2134.
- [19] Wegner, B., 2007. A Large-eddy simulation technique for the prediction of flow, mixing and combustion in gas turbine combustors. VDI-Verlag.
- [20] Werner, H., Wengle, H., 1993. Large-eddy simulation of turbulent flow over and around a cube in a plate channel, in: *Turbulent Shear Flows* 8. Springer, pp. 155–168.
- [21] Zimont, V., Polifke, W., Bettelini, M., Weisenstein, W., 1997. An efficient computational model for premixed turbulent combustion at high reynolds numbers based on a turbulent flame speed closure. *Journal of Engineering for Gas Turbines and Power* .